M&C 2017 - International Conference on Mathematics & Computational Methods Applied to Nuclear Science & Engineering, Jeju, Korea, April 16-20, 2017, on USB (2017)

Automated Inventory and Material Science Scoping Calculations under Fission and Fusion Conditions

Mark R. Gilbert, M. Fleming and J.-Ch. Sublet

United Kingdom Atomic Energy Authority, Culham Science Centre, Abingdon OX14 3DB, UK
mark.gilbert@ukaea.uk

Abstract - *The FISPACT-II inventory simulation platform is a modern computational tool with advanced and unique capabilities. It is sufficiently flexible and efficient to make it an ideal basis around which to perform extensive simulation studies to scope a variety of responses of many materials (elements) to several different neutron irradiation scenarios. This paper briefly presents the typical outputs from these scoping studies, which have been used to compile a suite of nuclear physics materials handbooks, providing a useful and vital resource for material selection and design studies. Several different global responses are extracted from these reports, allowing for comparisons between materials and between different irradiation conditions. A new graphical output format has been developed for the FISPACT-II platform to display these "global summaries"; results for different elements are shown in a periodic table layout, allowing side-by-side comparisons. Several examples of such plots are presented and discussed.*

I. INTRODUCTION

With the current maturity in nuclear inventory simulations it is also important to improve the way the results from the extensive output data sets are processed, analyzed and presented. In the past, only small amounts of data have been presented, usually for only one or two irradiation scenarios for a select few materials. Nowadays it is possible and routine to perform scoping calculations for many materials, for example the entire periodic table of elements, in multiple irradiation environments. The resulting data is vast and requires careful handling if the information is to be disseminated in an understandable and consistent manner. For this reason, the UKAEA, over a period of several years, has developed a suite of computational techniques that integrate with its own internationally recognised, modern inventory simulation platform FISPACT-II [1, 2]. These produce a variety of useful visual outputs to represent as much of the data as possible from single or multiple inventory simulations. This has culminated in the production of automatically-generated validation and verification reports [3, 4, 5] for the latest, modern nuclear data libraries TENDL-2015, ENDF/B-VII.1, JEFF-3.2 and JENDL-4.0u, as well as a new generation of extensive nuclear-physics materials handbooks [6, 7, 8, 9, 10, 11]. These handbooks, in particular, provide a huge wealth of information, scoping the radiological, transmutation (burn-up), and primary damage function responses for materials in typical fission reactor and predicted fusion environments. Furthermore the automated infrastructure, which efficiently creates and processes the tens of thousands of FISPACT-II & library inventory simulations required for the handbooks, can also be used to perform comparison studies by extracting the same response metric from the results of each material in a handbook and across multiple handbooks for nuclear library and/or environment. In this paper we briefly present the structure of the handbooks, before focussing on these comparisons for different response metrics.

II. CALCULATIONS AND PRESENTATION

For each handbook, an automated script runs, for each element or material, a sequence of simulated irradiations (followed by cooling as necessary) are performed for a set of incident neutron irradiation spectra (but focussing on one "main spectrum" for many outputs) using the FISPACT-II inventory code, and produces the outputs described below, which are fully described in, for example, [6]. Note that all results shown in the various example plots, and elsewhere in

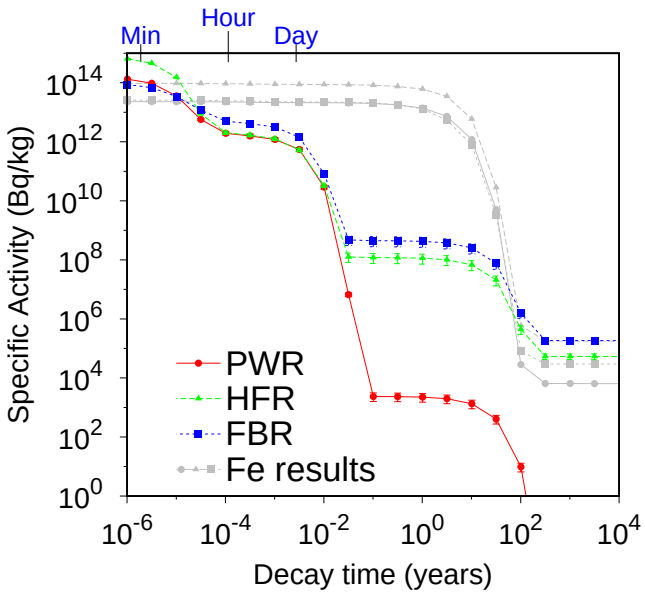

Fig. 1. Decay-cooling response of pure aluminium following 2 full-power year (fpy) irradiations under 3 typical fission scenarios: pressurized water-cooled reactor (PWR), the high-flux reactor (HFR) at Petten, and a fast-breeder reactor (FBR). The neutron flux spectra used are shown and described in more detail in Figure 3.

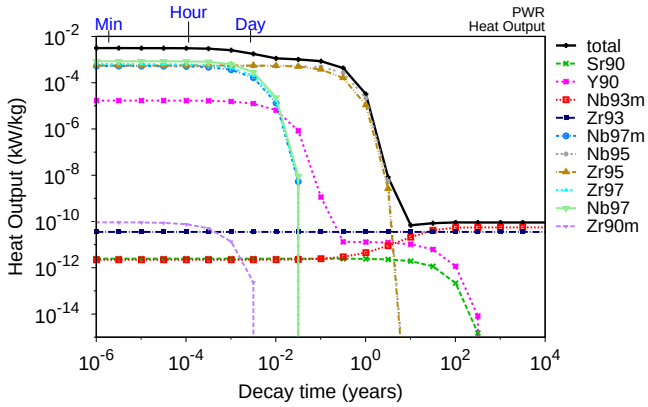

Fig. 2. Zr decay heat following 2 full-power years in a simulated fuel-assembly averaged neutron flux spectrum of a typical pressurized-water reactor (PWR) – see figure 3. The time-evolving decay-heat curves from the important contributing radionuclides are also shown, indicating which nuclides are important at different decay times.

this paper, were calculated by FISPACT-II using the TENDL-2015 [12] nuclear cross section libraries.

1. Activation tables – six tables, one for each of total (specific) activity (Bq kg^{-1}), decay heat (kW kg^{-1}), γ (contact) dose rate (Sv h^{-1}), inhalation and ingestion dose (Sv h^{-1}), and (IAEA) clearance index. Each table shows, for the primary irradiation spectrum of the handbook, the percentage contributions to the particular radiological response quantity at a range of cooling times following irradiations of typically 2 full power years (fpy), although for some applications the irradiation schedule can be more complex (see e.g. in [7], where materials were irradiated according to the planned 14-year operational scenario of the ITER experimental fusion reactor). The total radiological response is also given at each cooling time.

2. Activation graphs – three pairs of graphs, one for each of total activity, decay heat and γ dose rate. One graph shows the evolution in response of the material during cooling after the primary irradiation scenario of the handbook, together with result from several other irradiations (e.g. other fission reactors, or other reactor locations). For example, figure 1 shows the total becquerel activity response from pure aluminium following 2 fpy in the three typical fission neutron spectra shown in figure 3. Also shown in each such graph are equivalent results for pure Fe, providing a visual indication of the relative activity of a material compared to this standard material. The results in the figure demonstrate that irradiated Al is less active than Fe at most decay times, but also that Al is more activate (than Fe) at decay times greater than 100 years following irradiation in HFR and FBR conditions, due to subtle differences in the high neutron-energy profile of those neutron spectra compared to the PWR one (see figure 3). Note that nuclear cross section-based uncertainties are included as

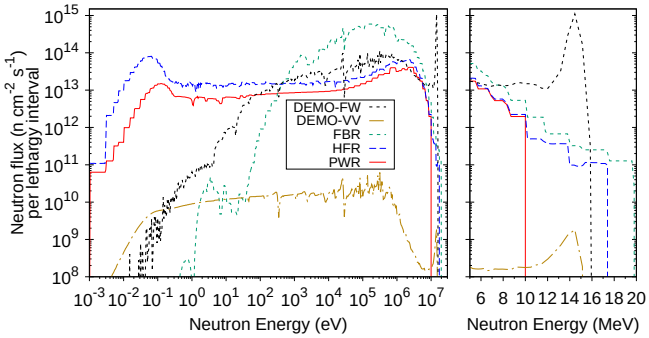

Fig. 3. Neutron spectra used for the scoping calculations, where DEMO-FW is a typical plasma-exposed, first wall spectrum for a demonstration fusion power plant (total integrated flux of 5.0×10^{14} n cm^{-2} s^{-1}); DEMO-VV is the equivalent spectrum predicted for the DEMO reactor vacuum vessel (2.5×10^{11} n cm^{-2} s^{-1}); FBR is the core assembly spectrum for the large-scale prototype fast breeder superphenix reactor that was located in the south of France (2.4×10^{15} n cm^{-2} s^{-1}); HFR is the spectrum for volume-averaged low-flux material test location of the high-flux reactor at Petten, Netherlands (5.3×10^{14} n cm^{-2} s^{-1}); and PWR is the fuel assembly-averaged spectrum for the type P4 pressurized-water reactor at the Paluel site in France (3.25×10^{14} n cm^{-2} s^{-1}). Left: the spectra on a logarithmic eV scale showing the full energy range. Right: a linear MeV scale, showing the high-energy parts of the spectra, in particular the fission tails.

standard in the graphs, but these are typically relatively small when viewed on the logarithmic scale of such plots (as in figure 1).
The second graph in the pair shows the response cooling following the main irradiation, but also includes an indication of which radionuclides are dominant for the radiological quantity at a particular cooling time. These are standard plots output from FISPACT-II (see [2] for details, but also the extensive use of such graphs in [5]). Nuclides appear at the position on the time (x) axis corresponding to their half-life and on the activity (y) axis corresponding to their contribution to the radiological quantity at shutdown after the irradiation.

3. Radionuclide contribution curves – three graphs, one for each of total activity, decay heat and γ dose rate. Each graph shows the cooling response for each radiological quantity following irradiation in the main spectrum of the handbook, but also includes the decay-cooling curves for the important radionuclides contributing to the total response (the same radionuclides included as labels in the activation plots described above). These graphs, which were newly developed in the FISPACT-II platform for the 2016 handbooks [6, 7], give a more easily interpretable (compared to other representations) visual of the important radionuclides as a function of time. Figure 2 shows such a graph for the decay heat from zirconium following a 2-fpy PWR irradiation. It is immediately possible to see the importance of the

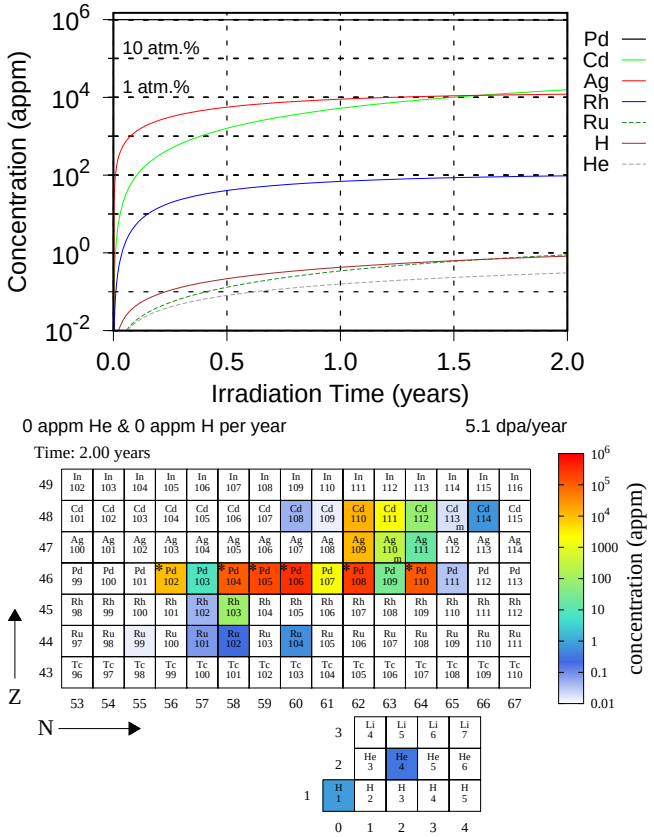

Fig. 4. Pd transmutation response under the irradiation conditions experienced in the high-flux reactor (HFR) in Petten, Netherlands (see Fig. 3). Top: elemental evolution in compositions (starting from 100% Pd) during 2 fpy. Bottom: Nuclide chart snapshot of isotopic composition after 2 fpy.

^{95}Nb and ^{95}Zr radionuclides on timescales between one day and 10 years following irradiation. In this particular example one can also observe the slight increase in decay heat from ^{93m}Nb ($T_{1/2}$ = 16.1 years) beyond 1 year due to the decay of the long-lived ^{93}Zr nuclide ($T_{1/2} = 1.5 \times 10^6$ years).

4. Importance diagrams [13, 14] – plots showing the regions of the incident-neutron-energy versus decay-time landscape where a single radionuclide dominates (contributes more than 50%) a particular activation quantity. These provide a general visual representation of the post-irradiation response of a material that is independent of any particular neutron spectrum, indicating the different radionuclides that are important in different neutron energy ranges and at what decay times. Diagrams for total activity, decay heat, and γ dose rate are produced by analyzing the output from a sequence of irradiations under mono-energetic (single energy group) neutron spectra.

5. Transmutation results – the burn-up response, where a material's composition changes with time due to irradiation, is calculated during irradiation and then plotted to show the growth of impurity elements, including gases

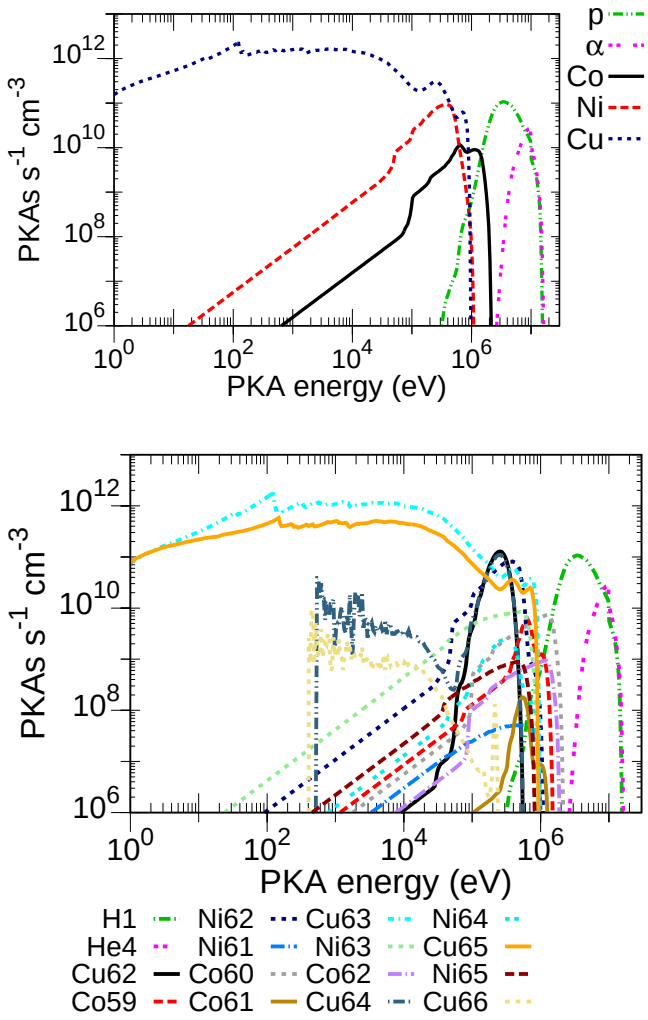

Fig. 5. Distributions of primary knock-on atom (PKA) rate spectra for pure copper under the irradiation conditions transmutation predicted for the first wall of a DEMO fusion power plant (see Fig. 3). Top: elemental sums. Bottom: Isotopic response. The per unit volume units were computed (from the raw PKs s^{-1} per target atom results) using the standard elemental density of Cu (8.96 g cm^{-3}).

He and H, and the corresponding depletion of the parent element. The He and H production in atomic parts per million (appm) in 1 fpy, and an estimate of the displacements per atom (dpa) per fpy, are output explicitly (as text). The final nuclide composition after the irradiation is also presented in a "chart of the nuclides" [14] tableau. Fig. 4 gives a typical result for this section – for pure palladium under HFR conditions. In this example, the overall transmutation burn-up of Pd is relatively small, with more than 97 atomic % of the Pd still remaining after 2 fpy. However, both Cd and Ag reach concentrations of more than 1%, although their isotopic distributions are somewhat different to that found naturally for those elements.

6. PKA distributions – primary knock-on atoms (PKAs) are the radiation damage source terms that determine the size of displacement damage cascades and hence the population of structural defects created in irradiated materials. They are important inputs to both atomistic simulations and the design of irradiation experiments. A newly written code, SPECTRA-PKA [15], combines (folds) an irradiation spectrum with neutron energy versus PKA recoil energy cross section (probability) matrices to define PKA-energy distributions for both nuclide (isotope) daughters and elemental recoil sums (more useful for atomistic modelling where different isotopes of the same element cannot normally be distinguished). For each handbook material, the isotopic and elemental-sum PKA spectra in units of PKA s^{-1} cm^{-3} are plotted for the main irradiation spectrum.
   Figure 5 shows the result for pure copper when irradiated in the typical fusion DEMO power plant plasma-exposed, first wall environment (see figure 3). As would be expected, the recoils of Cu itself are the most common due to the high probability of scattering. However, the high neutron energies of the fusion environment lead to the opening of additional reaction channels, where the recoiling particle is not necessarily Cu. These "none-Cu" recoils dominate the high recoil energy range (above 1 MeV), and will contribute non-negligibly to radiation damage, since such energetic particles create more damage than those at lower energies.

7. Pathway analysis – the important production pathways are calculated and output for every radionuclide considered significant because it appears in either the importance diagrams or activation tables of the element. A standard FISPACT-II pathway analysis (see [1] for details) is performed for the standard irradiation schedule of the handbook (typically 2 fpy) at a fixed neutron flux (typically 10^{15} n cm^2 s^{-1}) at four neutron energy ranges: thermal neutrons from 0.02 to 0.05 eV; intermediate neutrons from 20 to 40 keV; fast neutrons at typical fission energies of 1 to 3 MeV; and a fusion relevant range from 13 to 15 MeV. The output nuclides are listed in order of increasing decay half-life.

III. GLOBAL RESULTS

The main goal of the handbooks is to provide key response metrics for each naturally occurring element, so that their suitability for nuclear applications can be assessed. However, it is also useful to be able to collate results and compare certain responses across all elements in order to appreciate their relative behaviours. Such "global summaries" are relatively straightforward to produce using the automation developed to produce the suite of materials handbooks. An obvious way to present such comparisons is to follow the usual periodic table layout and use colouring to indicate the relative response of each element, which is also a natural extension of the techniques developed to present data on nuclide charts (see figure 4 and [14]).

Figure 6 shows the % burn-up or transmutation of each element per fpy under the predicted neutron spectrum and fluxes for the first wall environment of the 2014 European concept for a DEMOstration fusion power plant with a helium-cooled pebble-bed tritium-breeding blanket configuration (see [16, 17] for details). Only the naturally occurring elements from H to Bi are considered in the scoping calculations, so all other elements are white in the figure presentation (H and He are also white here because the transmutation rates are effectively zero). The figure provides a striking comparison between elements, showing outliers, such as the high burn-up of boron and indium, and low transmutation rates of bismuth and lead.

Another example is shown in figure 7, where the colouring this time reflects the simulated total becquerel activity from each elements 10 years after they have been irradiated for 2 fpy in the DEMO FW environment. Again, outliers are obvious, particularly cobalt, lithium and europium, and such a plot should prove very useful in material design studies – for example, as a quick reference to assess the likely impact (on activity) from adding certain elemental impurities to a composition.

1. Fusion vs. Fission Comparisons

A natural next step after producing the collated global results such as those described above is to use them to compare results from different scoping studies, i.e. from different handbooks. This is particularly useful when comparing results from different nuclear data libraries, because it can be used to identify discrepancies and deficiencies. However, it can also be used to compare results under different nuclear environments – for example comparing and contrasting nuclear fusion and fission.

Gas production is an important consideration in nuclear applications because gas build-up can severely reduce the working lifetime of materials, especially if accompanied by the in-growth of radiation-induced structural defects. Fig. 8 shows the helium gas production rates per displacements per atoms (dpa) – a useful damage dose measure – for all naturally occurring elements under fusion DEMO first wall [6] and the same fission conditions considered in [9, 10, 11], but instead computed using the latest TENDL-2015 [12] library. Fig. 3 shows the neutron spectra for the different environments considered. Note that ratios below 0.001 are omitted, and also that results for helium itself are not meaningful.

The results demonstrate the significantly higher ratios expected under fusion (DEMO) first wall conditions compared to fission for most materials, with many results for the fission scenarios not even appearing in the plots because they are too small. This result is entirely expected because many helium-producing nuclear reactions have energy thresholds, which sometimes means that they do not happen at all at fission-neutron energies, but are significant at the higher, fusion-neutron energies. This highlights that gas production is likely to be a more problematic phenomenon in fusion power plants (and also in advanced, fast fission reactors), and, further, that it is not straightforward to create suitable experimental test conditions in a fission reactor to reasonably approximate what a material will experience under fusion conditions.

Fig. 9 shows the total MBq kg^{-1} activity produced from

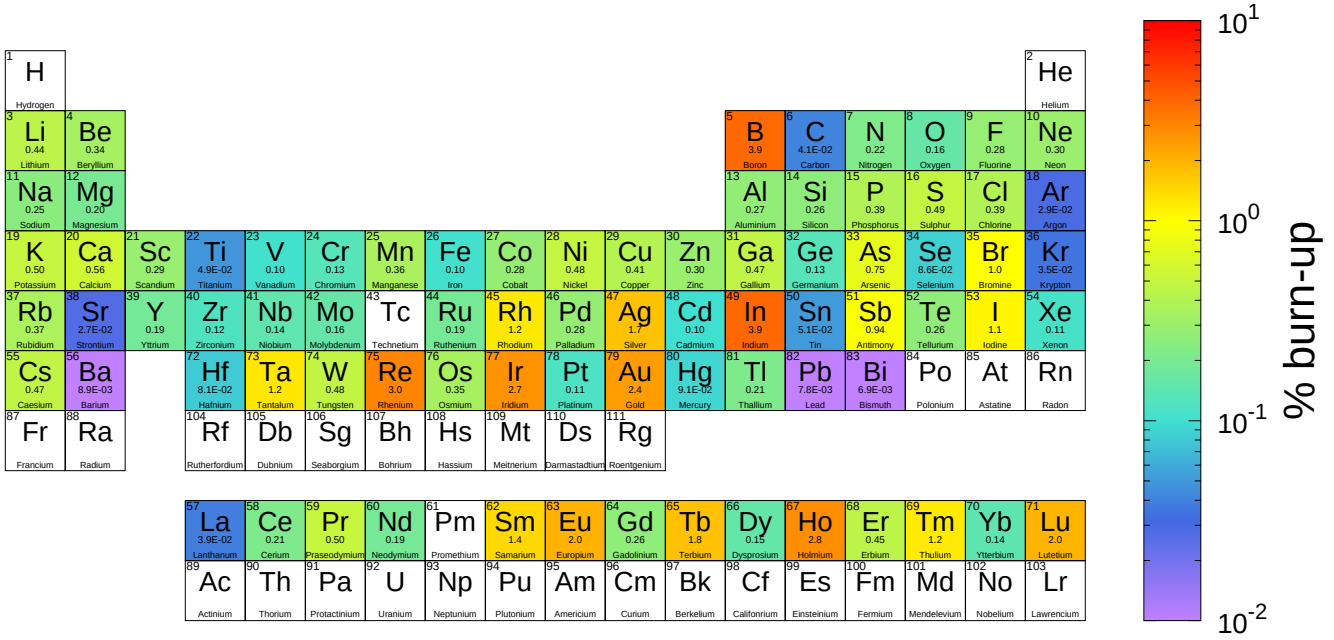

Fig. 6. % burn-up per fpy for each pure element under a fusion DEMO reactor plasma-exposed, first wall environment, whose neutron spectrum is shown in figure 3. The colour of each element depicts the burn-up (according to the associated logarithmic colour legend), but the absolute % values are also given beneath each element symbol.

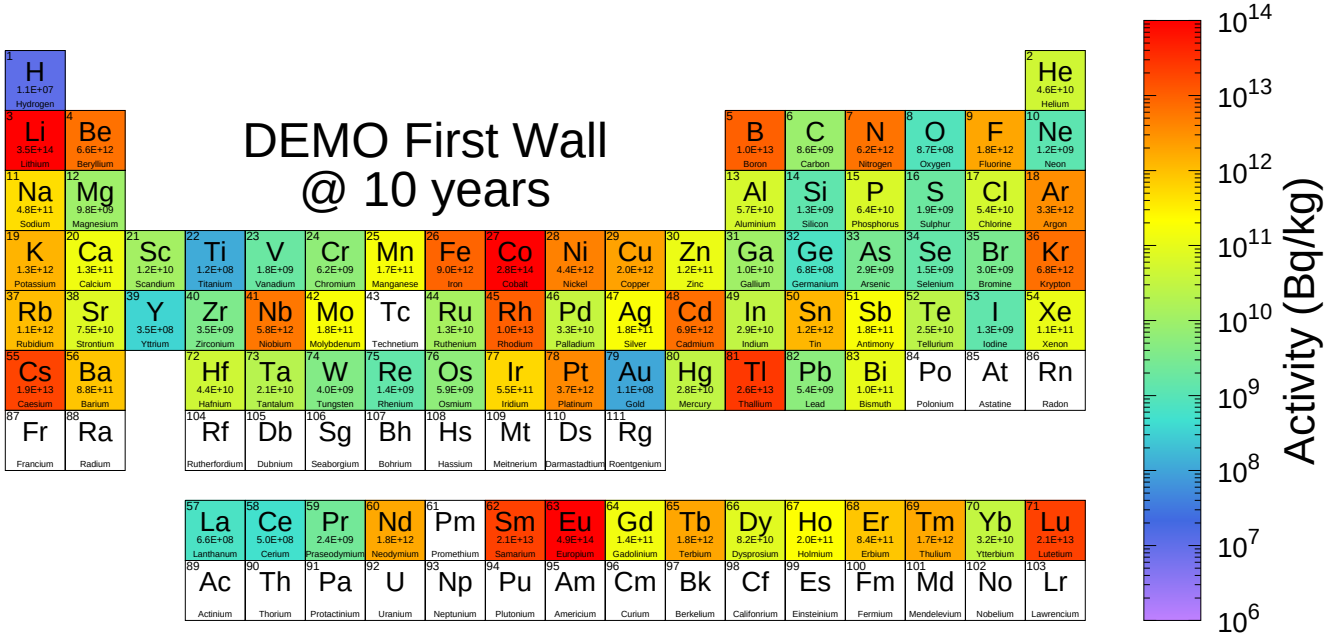

Fig. 7. Periodic table showing the total becquerel activity from each element after 10 years of decay cooling following a 2 fpy irradiation in a DEMO FW environment. The colour of each element reflects the activity according to the Bq kg^{-1} legend, but the absolute values are also given beneath each element symbol.

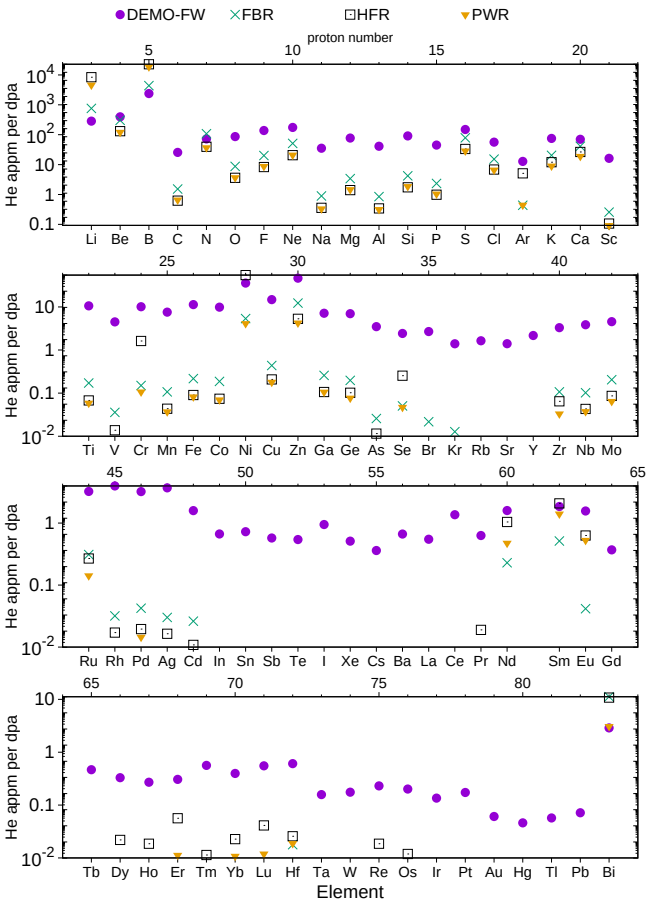

Fig. 8. Helium-to-dpa ratios for all naturally occurring elements (up to Bi) under a typical predicted fusion power plant (DEMO) first wall irradiation field compared to three fission environments: pressurized water-cooled reactor (PWR), the high-flux reactor (HFR) at Petten, and a fast-breeder reactor (FBR). All results were calculated by FISPACT-II using the TENDL-2015 [12] nuclear cross section libraries.

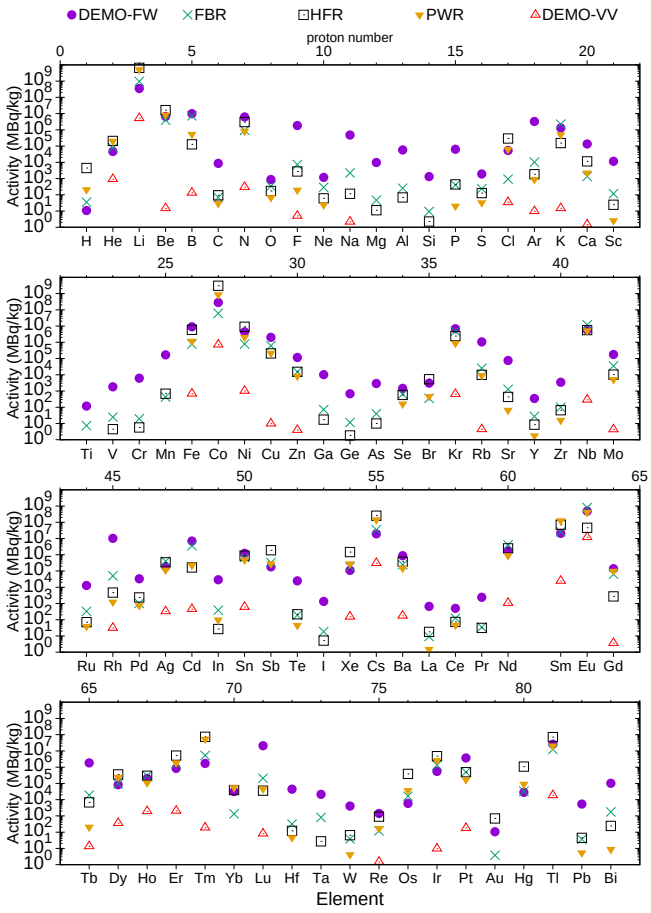

Fig. 9. Total activity 10 years after shutdown for all naturally occurring elements (up to Bi) after 2-fpy irradiations under typical fusion DEMO first wall (FW) and vacuum vessel (VV) irradiation fields compared to three typical fission environments.

each element 10 years after 2 fpy irradiations under both fusion and fission conditions. Here a cut-off at 1 MBq kg^{-1} has been used. In contrast to the He-to-dpa ratios in figure 8, the DEMO first wall environment is not the worst case for many elements, particularly in the higher proton number regions – although the relative comparisons vary significantly as a function of decay time (the DEMO-FW irradiations typically produce higher long-lived activity). The second set of fusion results plotted, that for the DEMO vacuum vessel (VV), are noticeably lower – lower even than the activation induced under fission conditions. This is perhaps highlighted even more clearly in the periodic-table graphic of these 10-year activation results for the DEMO-VV in figure 10, which uses the same colour scale as used for the previously discussed equivalent DEMO-FW results in figure 7.

It is obvious from the shift in the colouring of figure 10 to the "cooler" end of the spectrum in comparison to the FW results that the activation of materials in a DEMO VV will be significantly (many orders of magnitude) less, even allowing for the fact that VV materials will be expected to receive longer in-service exposure (in the scoping studies the irradiation times are kept fixed for ease of comparison). The comparison to the equivalent PWR results in figure 11 (again on the same colour scale) is similarly favourable for the VV, which is a significant portion of the total DEMO reactor mass [17]. This is an important exemplar of the commercial and political viability of fusion – even though certain in-vessel components will become significantly activated, many of the larger components will be less activated than under typical fission conditions.

IV. SUMMARY

Efficient computational automation of the running and processing of large-scale inventory simulation results provides a platform from which it is possible to explore the depths of modern nuclear data libraries and produce compilations of material responses that are invaluable to engineers, materials specialists, and other researchers working on the design and construction of the next generation of fission reactors and fusion experiments. It also provides a platform

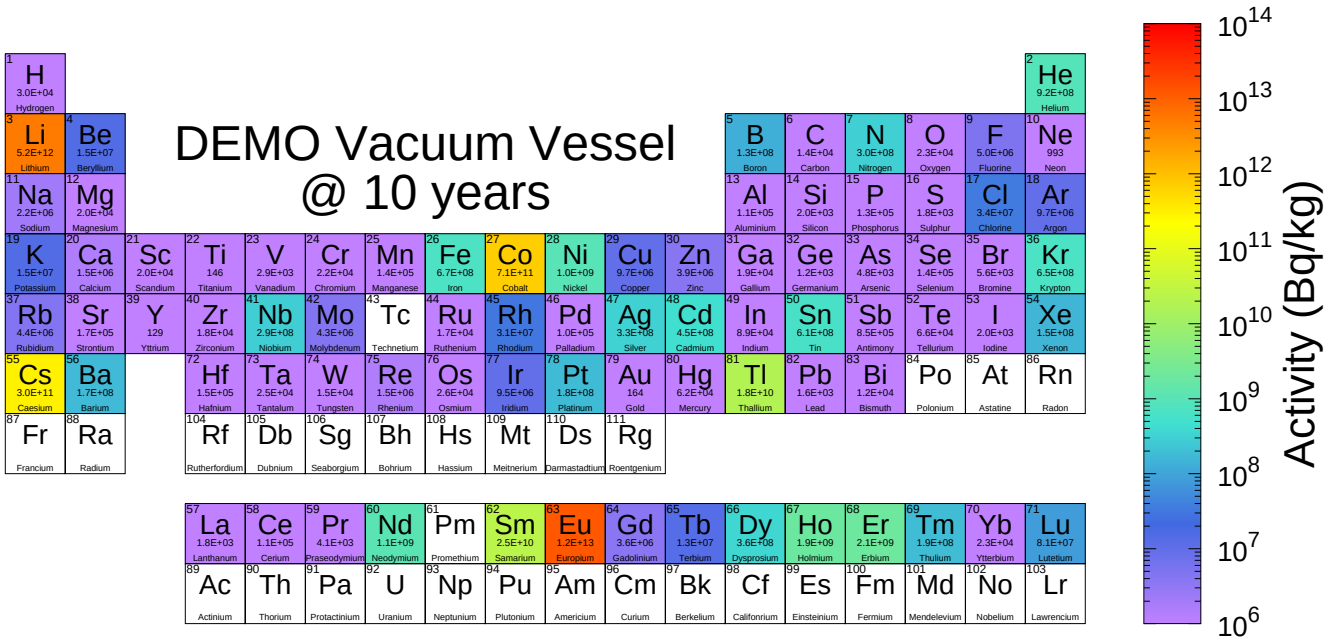

Fig. 10. Periodic table showing the total becquerel activity from each element after 10 years of decay cooling following a 2 fpy irradiation in a DEMO vacuum vessel (VV) environment. The colour of each element reflects the activity according to the Bq kg^{-1} legend, but the absolute values are also given beneath each element symbol.

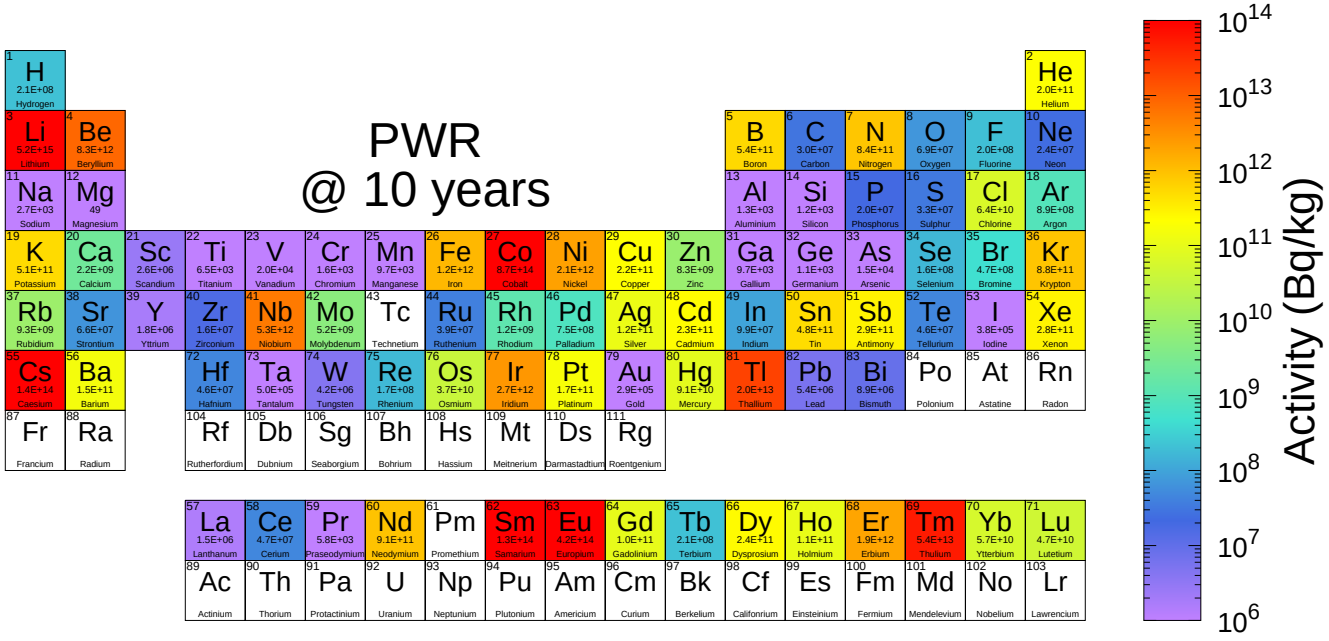

Fig. 11. Periodic table showing the total becquerel activity from each element after 10 years of decay cooling following a 2 fpy irradiation in a PWR fuel-assembly averaged environment. The colour of each element reflects the activity according to the Bq kg^{-1} legend, but the absolute values are also given beneath each element symbol.

to perform side-by-side comparisons, using innovative visual representations, of the response of different materials under a variety of irradiation conditions – allowing for new insights into the response landscape.

V. ACKNOWLEDGMENTS

This work was funded by the RCUK Energy Programme under grant EP/I501045. To obtain further information on the data and models underlying this paper please contact PublicationsManager@ccfe.ac.uk.

REFERENCES

1. J-CH. SUBLET, J. W. EASTWOOD, J. G. MORGAN, M. R. GILBERT, M. FLEMING, and W. ARTER, "FISPACT-II: An Advanced Simulation System for Activation, Transmutation and Material Modelling," *Nucl. Data Sheets*, **139**, 77–137 (2017), http://dx.doi.org/10.1016/j.nds.2017.01.002.
2. J.-C. SUBLET, J. EASTWOOD, J. MORGAN, M. FLEMING, and M. GILBERT, "FISPACT-II User Manual," Tech. Rep. UKAEA-R(11)11 Issue 8 (Dec. 2016), available from http://fispact.ukaea.uk.
3. M. FLEMING, J.-CH. SUBLET, and J. KOPECKY, "Integro-differential Verification and Validation, FISPACT-II & TENDL-2014 nuclear data libraries," Tech. Rep. CCFE-R(15)27, CCFE (2015), available from http://fispact.ukaea.uk.
4. M. FLEMING and J.-CH. SUBLET, "Validation of FISPACT-II decay heat and inventory predictions for fission events," Tech. Rep. CCFE-R(15)28, CCFE (2015), available from http://fispact.ukaea.uk.
5. J.-C. SUBLET and M. GILBERT, "Decay heat validation, FISPACT-II&TENDL-2014, JEFF-3.2, ENDF/B-VII.1 and JENDL-4.0 nuclear data libraries," Tech. Rep. CCFE-R(15)25, CCFE (2015), available from http://fispact.ukaea.uk.
6. M. R. GILBERT and J.-CH. SUBLET, "Handbook of activation, transmutation, and radiation damage properties of the elements simulated using FISPACT-II & TENDL-2015; Magnetic Fusion Plants," Tech. Rep. CCFE-R(16)36, CCFE (2016), available from http://fispact.ukaea.uk.
7. M. R. GILBERT, J.-CH. SUBLET, and A. TURNER, "Handbook of activation, transmutation, and radiation damage properties of the elements and of ITER materials simulated using FISPACT-II & TENDL-2015; ITER FW armour focus," Tech. Rep. CCFE-R(16) 37, CCFE (2016), available from http://fispact.ukaea.uk.
8. M. R. GILBERT, J.-CH. SUBLET, and R. A. FORREST, "Handbook of activation, transmutation, and radiation damage properties of the elements simulated using FISPACT-II & TENDL-2014; Magnetic Fusion Plants," Tech. Rep. CCFE-R(15)26, CCFE (2015), available from http://fispact.ukaea.uk.
9. M. R. GILBERT and J.-CH. SUBLET, "Handbook of activation, transmutation, and radiation damage properties of the elements simulated using FISPACT-II & TENDL-2014; Nuclear Fission plants (PWR focus)," Tech. Rep. UKAEA-R(15)31, UKAEA (2015), available from http://fispact.ukaea.uk.
10. M. R. GILBERT and J.-CH. SUBLET, "Handbook of activation, transmutation, and radiation damage properties of the elements simulated using FISPACT-II & TENDL-2014; Nuclear Fission plants (HFR focus)," Tech. Rep. UKAEA-R(15)32, UKAEA (2015), available from http://fispact.ukaea.uk.
11. M. R. GILBERT and J.-CH. SUBLET, "Handbook of activation, transmutation, and radiation damage properties of the elements simulated using FISPACT-II & TENDL-2014; Nuclear Fission plants (FBR focus)," Tech. Rep. UKAEA-R(15)33, UKAEA (2015), available from http://fispact.ukaea.uk.
12. A. J. KONING, D. ROCHMAN, J. KOPECKY, J-CH. SUBLET, M. FLEMING, E. BAUGE, S. HILAIRE, P. ROMAIN, B. MORILLON, H. DUARTE, S. VAN DER MARCK, S. POMP, H. SJOSTRAND, R. FORREST, H. HENRIKSSON, O. CABELLOS, S. GORIELY, J. LEPPANEN, H. LEEB, A. PLOMPEN, , and R. MILLS, "TENDL-2015," Release Date: January 18, 2016. Available from https://tendl.web.psi.ch/tendl_2015/tendl2015.html.
13. R. A. FORREST, "Importance diagrams — a novel presentation of the response of a material to neutron irradiation," *Fus. Eng. Des.*, **43**, 209–235 (1998), http://dx.doi.org/10.1016/S0920-3796(98)00418-9.
14. M. GILBERT, L. PACKER, J.-C. SUBLET, and R. FORREST, "Inventory simulations under neutron irradiation: visualization techniques as an aid to materials design," *Nuclear Science and Engineering*, **177**, *3*, 291–306 (2014), http://dx.doi.org/10.13182/NSE13-76.
15. M. GILBERT, J. MARIAN, and J.-CH. SUBLET, "Energy spectra of primary knock-on atoms under neutron irradiation," *J. Nucl. Mater.*, **467**, 121–134 (2015), http://dx.doi.org/10.1016/j.jnucmat.2015.09.023.
16. C. BACHMANN ET AL., "Initial DEMO tokamak design configuration studies," *Fus. Eng. Des.*, **98–99**, 1423–1426 (2015), http://dx.doi.org/10.1016/j.fusengdes.2015.05.027.
17. M. R. GILBERT, T. EADE, C. BACHMANN, U. FISCHER, and N. P. TAYLOR, "Activation, Decay Heat, and Waste Classification Studies of the European DEMO Concept," *Nucl. Fusion*, **57**, 046015 (2017), https://doi.org/10.1088/1741-4326/aa5bd7.